Unpromoted and K₂O-Promoted Cobalt Molybdate as Catalysts for the Decomposition of Acetic Acid

Samih A. Halawy[*]

Chemistry Department, Faculty of Science-Qena, South Valley University, Qena 83523, Egypt

Summary. Unpromoted cobalt molybdate was prepared from $Co(NO_3)_2 \cdot 6H_2O$ and $(NH_4)_6Mo_7O_{24} \cdot 4H_2O$, then calcined between 350 and 600°C for 5 h. K_2O (10 $w\%$), as a promoter, was added to the calcined sample at 350°C from two different sources (*i.e.* KOH and KNO_3) and was subjected to further calcination at 350°C for 5 h. The catalytic activity of unpromoted catalysts towards the vapour phase decomposition of CH_3COOH was greatly influenced by the increase in the calcination temperature. This is attributed to the diminution of both S_{BET} and their dual acidic–basic characters. The promoted sample from the KOH source was found to be the most active of the catalysts studied. This is due to its high population of both acidic–basic surface sites and the formation of two new phases. XRD and FTIR analyses of the used catalysts, after the decomposition reaction of acetic acid, showed a remarkable change in its structure compared with the parent samples.

Keywords. Acetic acid; Cobalt molybdate; K_2O; Catalytic properties.

Introduction

Co_3O_4–MoO_3 binary oxide mixtures, as pure or promoted with some alkali metal ions, have emerged as favorable catalysts in many areas of industrial applications. Syntheses of alcohols from CO_2/H_2 have been studied using this type of catalyst [1]. Many articles have examined the hydrodesulfurization power of different phases of $CoMoO_4$ and $NiMoO_4$ [2]. Other studies have dealt with the effect of potassium promotion on the activity of Co-containing catalysts during the combustion of diesel soot particles [3, 4], and *Fischer-Tropsch* synthesis over iron catalysts [5]. No methodical work has so far been published on acetic acid decomposition over unpromoted and K_2O-promoted $CoMoO_4$ catalysts. Decomposition of acetic acid in the gas phase can proceed via the following equation:

$$2CH_3COOH = CH_3COCH_3 + CO_2 + H_2O$$

[*] E-mail: shalawy99@yahoo.com

Several articles have been published on the catalytic wet oxidation (WO) of acetic acid on different types of catalysts [6–9]. Recently, some papers have been published on the ketonization of acetic acid using promoted modified zirconia [10] and some hydrotalcites [11] as catalysts.

The present work focused on measurement of the catalytic activity of unpromoted/K_2O-promoted $CoMoO_4$ during the decomposition of acetic acid in the gas phase. Identification of the different phases in the prepared samples as well as in the residual catalysts after the decomposition reaction were carried out using XRD and FTIR analyses, in order to get some information about the role of K_2O added as a promoter.

Results and Discussion

Powder X-Ray Diffraction

Figure 1 shows the XRD patterns of the calcination products of unpromoted cobalt molybdate at different temperatures. All samples are shown to consist of β-$CoMoO_4$ (ICDD 21-0868) and Co_3O_4 (ICDD 43-1003) as the main constituents together with α-$CoMoO_4$ (ICDD 25-1434) as a minor phase. As the calcination temperature increases from 350°C to 600°C, the content of α-$CoMoO_4$ decreases gradually as shown for those diffraction peaks at d-spacing = 1.924, 2.089, 2.726, 3.131, and 6.264 Å (ICDD 25-1434). The addition of K_2O to cobalt molybdate (from KOH and KNO_3) has resulted in the formation of new compounds in these two samples. Figure 2 displays the XRD patterns of CoMo–K_2O (hyd), CoMo–K_2O (nit) together with the original sample CoMo-350, all calcined at 350°C in air for 5 h. Appreciable amounts of both $K_2Co_2(MoO_4)_3$ and $K_2Mo_2O_7$ were formed as concluded from their diffraction lines at d-spacing = 1.946, 2.742, 2.979, 3.26, and 8.09 Å in case of $K_2Co_2(MoO_4)_3$ (ICDD 35-0070) and lines at 1.997, 2.096, 2.333, and 5.915 Å in case of $K_2Mo_2O_7$ (ICDD 36-0347).
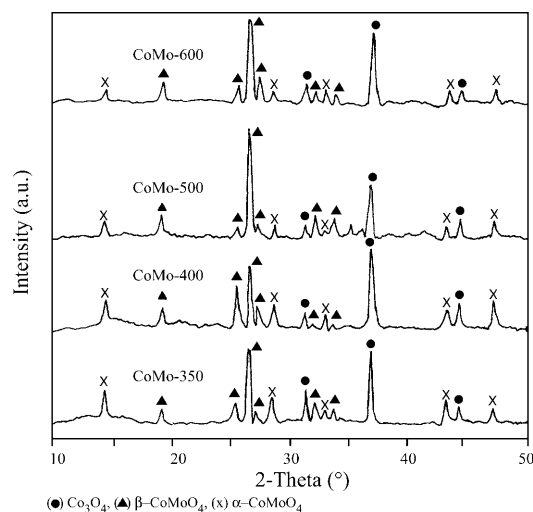

Fig. 1. XRD patterns of cobalt molybdate calcined at different temperatures for 5 h
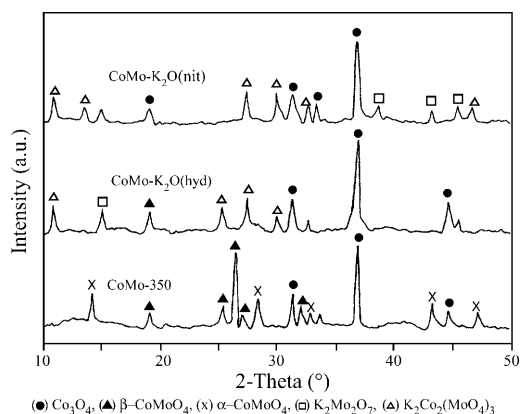
Fig. 2. XRD patterns of CoMo-350, K$_2$O-promoted catalysts CoMo–K$_2$O (hyd), and CoMo–K$_2$O (nit), calcined at 350°C for 5 h

Fourier Transform Infrared (FTIR) analysis

FTIR measurements were performed between 1200–300 cm^{-1}. The spectra of cobalt molybdate samples at different calcination temperatures were recorded. All spectra showed the same absorption bands of CoMoO$_4$ [16] located at 940–937, 863, 840, and 785 cm^{-1}. Two sharp absorption bands characteristic of Co$_3$O$_4$ [17] were shown at 660 and 566 cm^{-1}. In addition, a group of bands in the deformation mode of O–Mo–O [18] in the region 432–387 cm^{-1} was also shown. A weak shoulder appeared at *ca.* 996 cm^{-1} which was ascribed to the Mo=O
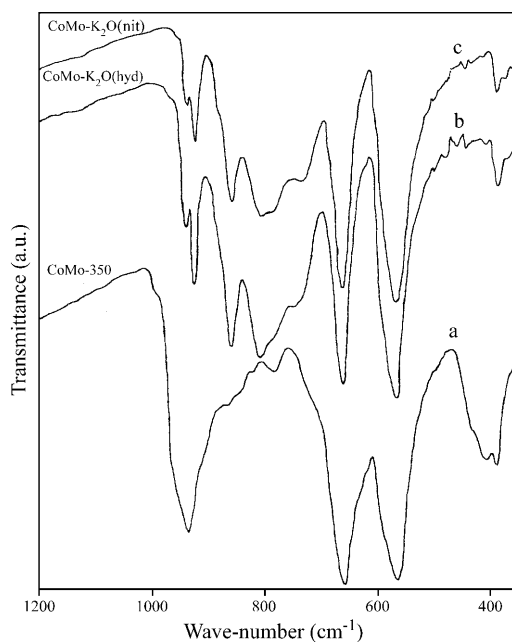

Fig. 3. FTIR spectra of (a) CoMo-350, K$_2$O-promoted catalysts, (b) CoMo–K$_2$O (hyd), and (c) CoMo–K$_2$O (nit), calcined at 350°C for 5 h

stretching mode [19]. Figure 3 represents the spectra of unpromoted CoMo-350 and CoMo–K$_2$O (hyd) together with CoMo–K$_2$O (nit), all were calcined at 350°C for 5 h in air. In addition to the above mentioned absorption bands, the spectra of K$_2$O-promoted samples, showed a different behaviour from the spectrum of CoMo-350 especially in the region 925–807 cm^{-1}. There are three new sharp absorption bands at 925, 860, and 807 cm^{-1} associated with the formation of K$_2$Mo$_2$O$_7$, as reported by *Erdőhelyi et al.* [20], while the absorption band of Mo=O was shifted towards a lower value (*i.e.* at 969 cm^{-1}) in case of CoMo–K$_2$O (hyd), CoMo–K$_2$O (nit). It is worth to note that the absorption band at 807 cm^{-1} in the spectra of the promoted catalysts indicates that Mo^{6+} ions are tetrahedrally coordinated [21]. The presence of K$_2$Co$_2$(MoO$_4$)$_3$ that was identified by XRD analysis (see Fig. 2) could not be confirmed by IR spectroscopy as there is no reference available for the absorptions of this compound.

XRD and FTIR analyses have supported the formation of β-CoMoO$_4$ and Co$_3$O$_4$ as main components in the unpromoted catalysts, besides the formation of two new phases K$_2$Mo$_2$O$_7$ and some K$_2$Co$_2$(MoO$_4$)$_3$ in the K$_2$O-promoted catalysts [1].

Decomposition of acetic acid

Unpromoted cobalt molybdate was found to exhibit a substantial activity towards the decomposition of acetic acid. Figure 4 represents the effect of calcination temperature on the catalytic activity of CoMo-catalysts during the gas phase decomposition of CH$_3$COOH. As the calcination temperature increases the activity of these catalysts decreases gradually. The catalyst calcined at 350°C, CoMo-350, was the most active one (conversion = 24.9%), while the catalyst calcined at 600°C, CoMo-600, was the least active catalyst (conversion = 6.4%). It is worth
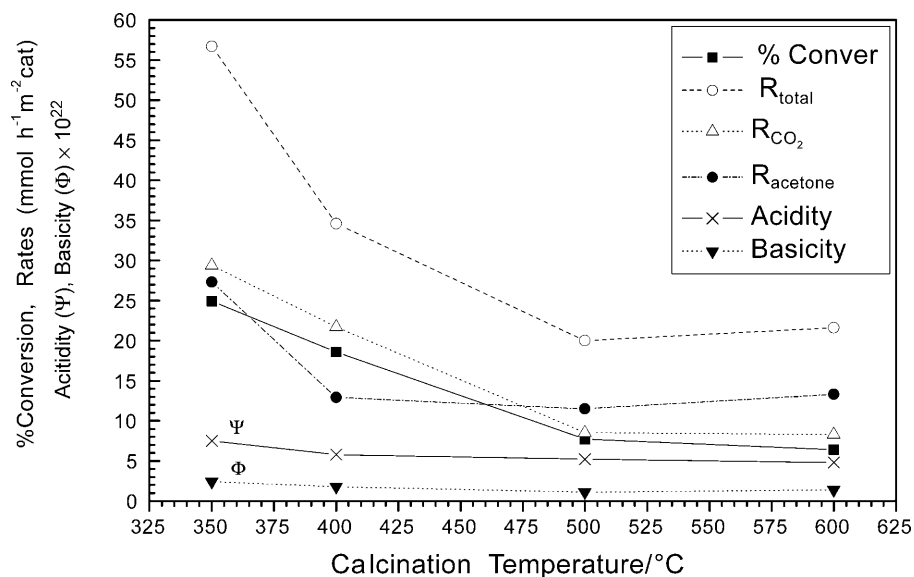

Fig. 4. Effect of calcination temperature on the catalytic activity, acidity, and basicity of unpromoted cobalt molybdate during acetic acid decomposition at 325°C

Table 1. Kinetic parameters of unpromoted/K$_2$O-promoted cobalt molybdates during the decomposition of acetic acid at 325°C as well as their S_{BET}, acidity, and basicity values

Sample	S_{BET} (m$^2 \cdot$ g^{-1})	% Conv.	R_{Total}[a]	$R_{acetone}$[a]	R_{CO_2}[a]	Acidity[b] $\Psi \cdot 10^{22}$	Basicity[c] $\Phi \cdot 10^{22}$
CoMo-350	18.8	24.9	56.7	27.3	29.4	7.5	2.4
CoMo-400	23.0	18.6	34.6	12.9	21.7	5.8	1.8
CoMo-500	16.5	7.7	20.0	11.5	8.5	5.2	1.1
CoMo-600	12.7	6.4	21.6	13.3	8.3	4.8	1.4
CoMo–K$_2$O$_{hyd}$	5.6	29.4	222.2	85.1	137.1	27.7	35.6
CoMo–K$_2$O$_{nit}$	6.0	26.1	178.7	69.9	108.8	17.7	32.6

[a] Rate = mmol h^{-1} m$^{-2}_{catalyst}$; [b] Ψ = acidity (sites m$^{-2}_{catalyst}$); [c] Φ = basicity (sites m$^{-2}_{catalyst}$)

noting that R_{total} (the total rate of acetic acid decomposition) decreased gradually until CoMo-500, and then increases slightly at CoMo-600. Similarly, $R_{acetone}$ (the rate of acetone formation) behaves as R_{total}. This is due to a slight increase in population of the basic sites of this catalyst CoMo-600 (see Table 1). While molybdates are known to possess fairly acidic characters [18, 22], Co_3O_4 possesses a higher basic site concentration relative to the acidic sites [23]. Therefore, all CoMo-catalysts showed more acidity than basicity population. Consequently, both $R_{acetone}$ and R_{CO_2} (rate of CO_2 formation) have comparatively high values, see Table 1.

The promotion effect of K$_2$O added to the CoMo-catalyst from two different sources was studied. The results are presented in Fig. 5. As the reaction temperature increases the catalytic activity of K$_2$O-promoted catalysts was always higher than that of the unpromoted sample. A significant increase in the conversion was
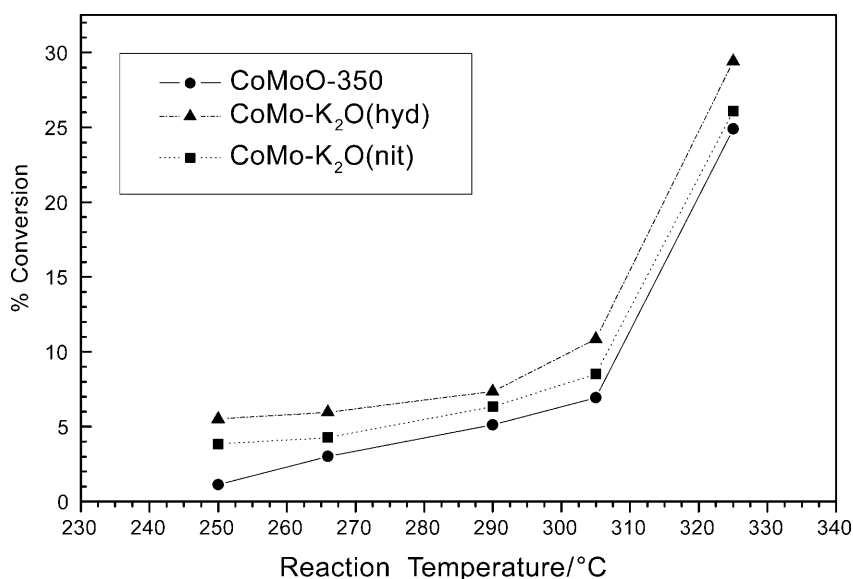

Fig. 5. Conversion of acetic acid as a function of reaction temperature over CoMo-350, CoMo–K$_2$O (hyd), and CoMo–K$_2$O (nit), all calcined at 350°C for 5 h
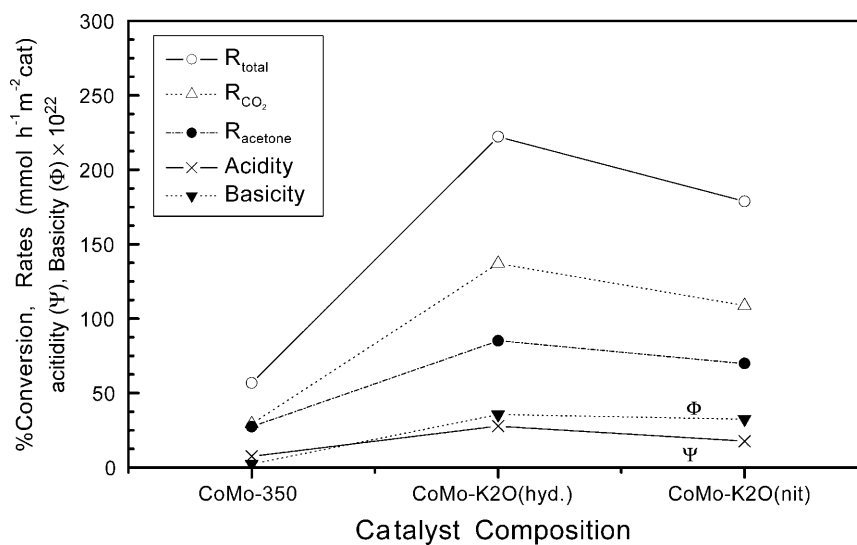
Fig. 6. Catalyst composition as a function of acidity–basicity and activity of unpromoted/K_2O-promoted catalysts during acetic acid decomposition at 325°C

observed for the three catalysts in the following order when the reaction temperature was increased from 250 to 325°C: CoMo–K_2O (hyd) > CoMo–K_2O (nit) > CoMo-350. This can be correlated with the dual acidic–basic characters of these catalysts. The addition of K_2O resulted not only in the formation of more acidic M^{6+} species [24] due to the formation of $K_2Mo_2O_7$ and $K_2Co_2(MoO_4)_3$ (see Fig. 2), but also in more basic sites of K^+ ions in these promoted catalysts. Therefore, the population of both acidic and basic sites were increased significantly, see Table 1 and Fig. 6. The catalyst CoMo–K_2O (hyd) exhibited the highest reactivity of all the studied catalysts. This is clear from the values of R_{total}, $R_{acetone}$, and R_{CO_2} of this catalyst, see Table 1 and Fig. 6. This is due to the higher dual acidic–basic characters of this catalyst compared with the other promoted catalyst CoMo–K_2O (nit). Finally, the unpromoted CoMo-350 has the smallest rate values.

In order to identify the residual catalysts after acetic acid decomposition of the unpromoted CoMo-350 and the most active catalyst CoMo–K_2O (hyd), XRD and FTIR analyses were performed for the used catalysts and were compared with the fresh samples. Figure 7 shows the XRD patterns of the fresh samples of CoMo-350 and CoMo–K_2O (hyd) together with the used catalysts after the reaction. An important observation is the strong peak at $d = 2.443$ Å, while the other two peaks at 2.025 and 2.857 Å, assigned to Co_3O_4 (ICDD 43-1003), have completely vanished after the decomposition of acetic acid (see the pattern of the used catalyst). On the other hand, a new peak appeared in the XRD pattern of the used CoMo-350 at $d = 2.129$ Å due to CoO (ICDD 9-0402). Another peak appeared in the XRD pattern of the used sample of CoMo–K_2O (hyd) at $d = 2.457$ Å associated with the formation of $K_2Co_2(MoO_4)_3$ (ICDD 35-0070). To confirm the XRD observations, FTIR analyses of the same samples were carried out (Fig. 8). Spectrum (a) of unpromoted CoMo-350 shows that the characteristic strong bands at 660 and 565 cm^{-1} due to Co_3O_4 [17] have completely vanished. After the catalytic
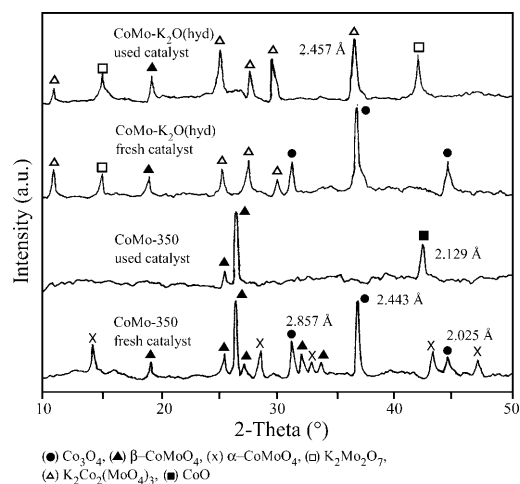
Fig. 7. XRD patterns of fresh and used catalysts after the decomposition of acetic acid, of CoMo-350 and CoMo−K₂O (hyd)
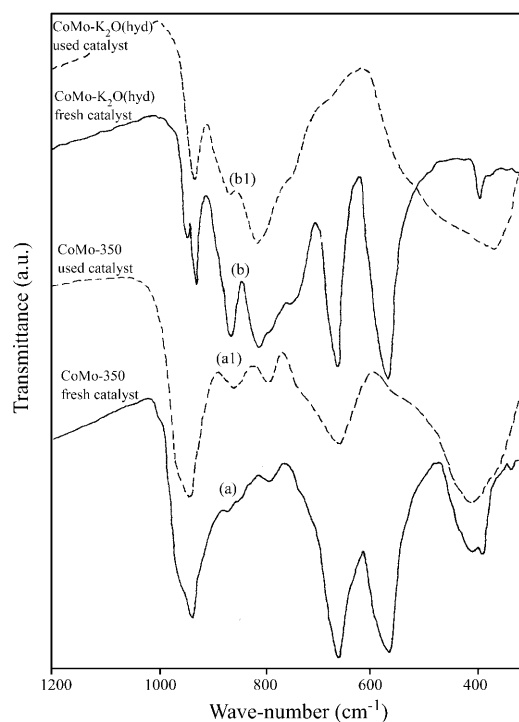

Fig. 8. FTIR spectra of fresh and used catalysts after the decomposition of acetic acid, of CoMo-350 and CoMo−K₂O (hyd)

decomposition of acetic acid, the IR spectrum (a1) of the used catalyst CoMo-350 shows two broad peaks located at 653 and 408 cm^{-1} ascribed to CoO [25]. Absorption bands of $CoMoO_4$ remained unchanged. For spectrum (b) of the fresh

sample of CoMo–K_2O (hyd), the comparison between the IR spectra of the promoted catalyst, CoMo–K_2O (hyd), before and after the catalyzed decomposition of acetic acid revealed two differences:

(i) three absorption bands have completely disappeared in the spectrum of the used catalyst (b1) at $940\,cm^{-1}$ (of $CoMoO_4$) and at 661 and $568\,cm^{-1}$ (bands of Co_3O_4), and

(ii) the intensity of the band at $858\,cm^{-1}$ of $K_2Mo_2O_7$ [20] has notably been reduced.

From the two differences, one can conclude that in the promoted catalyst, CoMo–K_2O (hyd), Co_3O_4 has been completely reduced to CoO. The presence of K^+ ions in $K_2Mo_2O_7$ facilitate the interaction between CoO and $CoMoO_4$ to form $K_2Co_2(MoO_4)_3$, see XRD Fig. 7.

Conclusions

(i) Cobalt molybdate catalysts were prepared from $Co(NO_3)_2 \cdot 6H_2O$ and $(NH_4)_6Mo_7O_{24} \cdot 4H_2O$, and were calcined between 350 and 600°C. Catalyst samples were shown to contain a mixture of β-$CoMoO_4$ and Co_3O_4 as main components, where $\alpha \rightarrow \beta$ transition of $CoMoO_4$ is known to occur between 330 and 410°C [26].

(ii) As the calcination temperature increased, the activity of cobalt molybdate catalysts decreased gradually. This is due to the shrinking of their surface area and, consequently, the reduction of their acidic–basic sites.

(iii) The addition of K_2O from two sources to $CoMoO_4$ has resulted in the formation of two new phases, *i.e.* $K_2Mo_2O_7$ and $K_2Co_2(MoO_4)_3$.

(iv) The promoted catalyst, CoMo–K_2O (hyd), was the most active catalyst studied. It was characterized by a high concentration of the basic centers whereas its acidic sites played a less important role.

(v) The surface area was an effective parameter in addition to the dual acidic–basic characters of the unpromoted $CoMoO_4$. This factor, however, was less important in case of K_2O-promoted catalysts. This could be due to potassium which is reported [3] to cause a strong decrease in the specific surface area of these catalysts. On the other hand, it is concluded from XRD and FTIR analyses of the fresh and used catalysts that K^+ plays an important role in the activity of the promoted catalysts by preserving the redox capacity of cobalt [4] in $CoMoO_4$.

(vi) β-$CoMoO_4$ or K_2O-promoted $CoMoO_4$ were shown to be weak catalysts for ketonization of acetic acid. This could be due to their dual acidic–basic properties, while ketonization of acetic acid, on the other hand, is known to require fairly basic catalysts [11].

Experimental

Preparation of the catalyst samples

The unpromoted sample of cobalt molybdate was prepared by dissolving 87.3 g of $Co(NO_3)_2 \cdot 6H_2O$ (BDH) in a sufficient amount of deionized water, then 17.7 g of $(NH_4)_6Mo_7O_{24} \cdot 4H_2O$ (Fisions) was

suspended in this solution. The mixture was then evaporated to dryness with continuous stirring over a water bath. The resulting material was dried at 120°C in an oven for 24 h. Finally, portions of the catalyst were calcined in air for 5 h at 350, 400, 500, and 600°C. K$_2$O-promoted samples, denoted as CoMo–K$_2$O (hyd) and CoMo–K$_2$O (nit), were prepared by the wet impregnation method. 10 w% K$_2$O was added to 1.8 g of CoMo-350, the calcined sample of cobalt molybdate at 350°C, from two sources (0.24 g KOH (BDH) and 0.43 g KNO$_3$ (BDH)) respectively, using few drops of deionized water. The resulting homogeneous pasts were then dried and recalcined again at 350°C in air for 5 h.

Characterization

X-ray powder diffractograms (XRD) of the catalysts and two used catalysts were measured using a D5000 Siemens diffractometer (Germany) at ambient temperature. The instrument used Ni-filtered CuK$_\alpha$ radiation ($\lambda = 1.5418$ Å, 40 kV, 30 mA). IR spectra of the unpromoted CoMoO$_4$/K$_2$O-promoted CoMoO$_4$ catalysts as well as two used catalysts were recorded by the KBr disk technique using a Magna-FTIR-560 (USA) instrument operated by Nicolet Omnic software. The BET surface area was obtained from nitrogen adsorption isotherms measured at liquid nitrogen temperature with an automatic ASAP 2010 Sorptometer Micromeritics (USA). The total surface basic–acidic sites of the catalysts were measured by temperature-programmed desorption of formic acid and pyridine, respectively [12, 13]. The population of both surface acidic (Ψ) and basic sites (Φ) were determined thermogravimetrically [14] as follows: 100 mg portions of each sample were heated at 250°C in air for 2 h, then kept in a desiccator together with an open beaker containing pyridine or formic acid at ambient temperature for two weeks, prior to analysis. A 15-mg portion of each pyridine or formic acid-covered sample was subjected to TG analysis on heating up to 350°C (at 20°C/min) in dry N$_2$ (40 ml/min) using an automatically recording Shimadzu Stand-Alone TGA-50H (Japan). The weight loss, due to the desorption of pyridine and formic acid from the acidic and basic sites, was determined as a function of both the acidity and the basicity of these catalysts.

Decomposition of acetic acid

The catalytic activity of all catalysts towards the decomposition of acetic acid was determined in the gas phase in a fixed bed reactor. All experiments were conducted at atmospheric pressure in a continuous flow mode, using a mixture of 0.74% CH$_3$COOH in dry N$_2$, obtained by passing N$_2$ through liquid acetic acid (Prolabo) in a saturator at 10°C. The total flow rate 147.7 cm^3 (STP) min^{-1} was composed of 1.1 cm^3 (STP) CH$_3$COOH and 146.6 cm^3 (STP) min^{-1} dry N$_2$. A catalyst sample of 100 mg was stabilized in a Pyrex glass reactor for 1 h at 200°C before measurements in a stream of dry N$_2$. The reactor effluent was analyzed by a gas chromatograph (Shimadzu GC-14A) equipped with a data processor model Shimadzu Chromatopac C-R4AD (Japan). TCD and SUS, PEG 6000 10% on Shimalite TPA, 60/80 mesh (3 mm i.d.×2 m) column at 150°C were used. Automatic sampling was performed with a heated gas sample cock, type HGS-2. The retention time of acetic acid as a reactant, and the expected decomposition products (CO$_2$ and CH$_3$COCH$_3$) have been calibrated in separate experiments using pure authentic specimens. Conversion (%) and reaction rates during the decomposition of CH$_3$COOH were calculated as explained in detail recently [15].

References

[1] Calafat A, Vivas F, Brito JL (1998) Appl Catal A **172**: 217
[2] Rodriguez JA, Chaturvedi S, Hanson JC, Brito JL (1999) J Phys Chem B **103**: 770
[3] Querini CA, Ulla MA, Requejo F, Soria J, Sedrán UA, Miró EE (1998) Appl Catal B **15**: 5
[4] Querini CA, Cornaglia LM, Ulla MA, Miró EE (1999) Appl Catal B **20**: 165
[5] Eliason SA, Bartholomew CH (1999) Appl Catal A **186**: 229
[6] Klinghoffer AA, Cerro RL, Abraham MA (1998) Catal Today **40**: 59

[7] Gallezot P, Chaumet S, Perrard A, Isnard P (1997) J Catal **168**: 104

[8] Shende RV, Mahajani VV (1997) Indst & Eng Chem Res **36**: 4809

[9] Yu J, Savage PE (2000) Indst & Eng Chem Res **39**: 4014

[10] Parida K, Mishra HK (1999) J Mol Catal A **139**: 73

[11] Parida K, Das J (2000) J Mol Catal A **151**: 185

[12] Fung J, Wang I (1998) Appl Catal A **166**: 327

[13] Iengo P, Di Serio M, Sorrentino A, Solinas V, Santacesaria E (1998) Appl Catal A **167**: 85

[14] El-Katatny EA, Halawy SA, Mohamed MA, Zaki MI (2000) Appl Catal A **199**: 83

[15] Abd El-Raady AA, Fouad NE, Mohamed MA, Halawy SA (2002) Chem Monthly **133**: 1351

[16] Cord PP, Courtine P, Pannetier G, Guillermet J (1972) Spectrochim Acta **28A**: 1601

[17] Bentley FF, Smithson LD, Rozek AL (1968) Infrared spectra and characteristic frequencies $\sim$700–300 cm^{-1}, Wiley, New York, p 103

[18] Al-Shihry SS, Halawy SA (1996) J Mol Catal A **113**: 479

[19] Hiratta T, Fukuda Y (1990) J Mater Sci Lett **9**: 929

[20] Erdőhelyi A, Fodor K, Solymosi F (1997) J Catal **166**: 244

[21] Giordano N, Bart JCJ, Vaghi A, Castellan A, Martinotti G (1975) J Catal **36**: 81

[22] Halawy SA, Al-Shihry SS (1999) J Therm Anal & Calorim **55**: 833

[23] Bezouhanova CP, Al-Zihari MA (1991) Catal Lett **11**: 245

[24] Martín C, Martín I, del Moral C, Rives V (1994) J Catal **146**: 415

[25] Nyquist RA, Kogal RO (1971) Infrared spectra of inorganic compounds, Academic Press, New York, p 219

[26] Rodriguez JA, Chaturvedi S, Hanson JC, Albornoz A, Brito JL (1998) J Phys Chem B **102**: 1347